

OPTIMAL LARGE ANGLE MANEUVERS  
WITH SIMULTANEOUS SHAPE CONTROL/VIBRATION ARREST

James D. Turner and John L. Junkins  
Virginia Polytechnic Institute and State University

ABSTRACT

A relaxation method is demonstrated which reliably solves the nonlinear two-point-boundary-value problem which arises when optimal control theory is applied to determination of large angle maneuvers of flexible spacecraft. The basic ideas are summarized and several idealized maneuvers are determined. The emphasis is upon demonstrating the basic ideas and practical aspects of the methodology. References are cited, particularly Turner's dissertation which presents detailed formulations and more general applications.

## Discussion of Figures

With reference to Figure 1, we employ the method of assumed modes to obtain a set of ordinary differential equations which govern deflections and rotations. The form of the equations of motion are given in Figure 2. Note the high dimensionality and the variability of the coefficient matrix. Note that solution for the acceleration coordinates is required in order to integrate motion as a function of time, and in order to apply optimal control theory.

Figure 3 displays a partitioned algorithm which efficiently determines the inverse of the high-dimensional, configuration-variable coefficient matrix. Consistent with this partitioning algorithm, we consider in Figure 4 an algorithm for obtaining partial derivatives of the inverted coefficient matrix with respect to deflection coordinates (required in the optimal control algorithm).

Figure 5 summarizes the state and co-state differential equations which follow from Pontryagin's principle as the necessary conditions satisfied by optimal (minimum quadratic cost) maneuvers. Observe that the initial and final states are generally known, but the initial and final co-states are usually unknown. Thus, as usual, a nonlinear two point boundary value problem (TPBVP) has resulted. Notice the quadratic angular velocity nonlinearity due to "rotational stiffness."

In Figure 6, we summarize an imbedding/relaxation approach which has proven a reliable approach for solving TPBVP's of the above structure. In essence, a one parameter ( $\alpha$ ) family of problems is constructed that one special member ( $\alpha = 0$ ) has an analytical solution, while another member ( $\alpha = 1$ ) is the true problem of interest. By relaxing  $\alpha$  through a sequence of increasing values  $0 \leq \alpha_j \leq 1$ , we can extrapolate arbitrarily good initial or final co-state estimates (by adjusting the  $\alpha$ -increment) from previous converged solutions, thereby allowing efficient differential corrections to isolate accurate co-states corresponding to each  $\alpha$ . Typically, only 4 or 5  $\alpha_j$  values are actually required to reach the desired  $\alpha = 1$  solution. This method and related methods are developed and applied to several examples in Reference 3.

Considering now a specific configuration, we refer to Figure 7. The four identical cantilevered appendages are mounted in the same plane to the rigid central hub. We neglect the hub radius in any equation in which it appears divided by the appendage length. Referring to Figure 8, we restrict attention to pure spin rotations and antisymmetric deflections, consistent with spin-up, spin-down, and rest-to-rest maneuvers with the configuration initially and finally undeformed. We consider only the case of torques applied to the hub.

Table 1 describes seven maneuver calculations, corresponding to three sets of maneuver boundary conditions and four different dynamical models. These cases are selected to demonstrate the effects of rotational stiffening and to show that the relaxation method can handle both high dimensionality and nonlinearities.

Figures 9a - c display the angle of rotation, angular rate and torque for the case 1 maneuver (rigid appendages). For comparison, Figures 10a - c display the same variables for cases 2L and 2N of flexible appendages, assuming a 1 mode expansion. It is of interest to note that the flexibility

effects are large indeed. The flexible case torque oscillates anti-symmetrically about the rigid case torque, the desired final angle and angular rate are achieved and the modal amplitude (and its derivative) are simultaneously driven to zero. It is interesting that the linear and nonlinear solutions were identical, to graphical accuracy, due to the small deflections and velocities of this particular maneuver.

Figure 11a – d and 12a – d display angle of rotation, torque history, and amplitudes of the first two modes for cases 3L and 3N, respectively. The maneuver is an extremely rapid spinup from rest to 0.5 rad/sec in 60 sec. The linear (3L) and nonlinear (3N) solutions differ significantly, but the linear solution retains the general shape and amplitudes differ by less than 10% throughout most of the motion.

Figure 13a – g display the angle of rotation, angular rate, torque, and the first four modal amplitudes for case 4L (a rest-to-rest maneuver through a 360° rotation). These results simply show that, indeed, the large rigid rotations and vibration suppression of several degrees of freedom are determined.

We offer the following significant conclusions:

- An Optimal Control Formulation is Presented for General 3 Dimensional Maneuvers of a Class of Flexible Satellites
- A Partitioning Method is Introduced to Invert the Rotational-Vibrational Equations of Motion for Acceleration Coordinates and to Obtain the Adjoint Equations
- An Imbedding/Relaxation Process is Demonstrated for Solution of the Two-Point-Boundary-Value Problem.
- Numerical Studies Indicate that Practical Algorithms Result from these Developments

#### References

1. Junkins, J.L. and J.D. Turner, "Optimal Continuous Torque Attitude Maneuvers," AIAA preprint #78-1400, presented to the AIAA/AAS Astrodynamics Conference, Palo Alto, CA., August 1978; also, to appear, AIAA Journal of Guidance and Control.
2. Turner, J.D. and J.L. Junkins, "Optimal Large Angle Single Axis Rotational Maneuvers of Flexible Spacecraft," presented to the 2nd AIAA/VPI&SU Symposium on Dynamics and Control of Large Flexible Spacecraft, Blacksburg, VA., June 1979, proceedings in press; also, to appear in AIAA Journal of Guidance and Control.
3. Turner, J.D. "Optimal Large Angle Maneuvers for Large Flexible Space Structures," Ph.D. Dissertation, Virginia Polytechnic Institute and State University, Blacksburg, VA., in press.

## THE METHOD OF ASSUMED MODES

The deflection of the  $j$ th flexible member is modeled as

$$\left. \begin{aligned}
 u_j(x, y, z, t) &= \sum_{i=1}^{L_j} \alpha_{ji}(t) & U_{ji}(x, y, z) &= \underline{\alpha}_j^T \underline{U}_j \\
 v_j(x, y, z, t) &= \sum_{i=1}^{M_j} \beta_{ji}(t) & V_{ji}(x, y, z) &= \underline{\beta}_j^T \underline{V}_j \\
 w_j(x, y, z, t) &= \sum_{i=1}^{N_j} \gamma_{ji}(t) & W_{ji}(x, y, z) &= \underline{\gamma}_j^T \underline{W}_j
 \end{aligned} \right\} j=1, 2, \dots, n \quad (1)$$

The sets of spatial "assumed modes"

$$\begin{aligned}
 &\{ U_{11}(x, y, z) \dots U_{1i}(x, y, z) \} \dots \{ U_{n1}(x, y, z) \dots U_{ni}(x, y, z) \} \\
 &\{ V_{11}(x, y, z) \dots V_{1i}(x, y, z) \} \dots \{ V_{n1}(x, y, z) \dots V_{ni}(x, y, z) \} \\
 &\{ W_{11}(x, y, z) \dots W_{1i}(x, y, z) \} \dots \{ W_{n1}(x, y, z) \dots W_{ni}(x, y, z) \}
 \end{aligned}$$

are prescribed. As minimum requirements, they must

- be linearly independent
- satisfy  $u, v, w$ 's geometric boundary conditions

The amplitude functions constitute the *configuration vector*  $\underline{n}(t)$

$$\underline{n}(t) = \{ \underline{\alpha}_1^T, \underline{\beta}_1^T, \underline{\gamma}_1^T; \dots \underline{\alpha}_n^T, \underline{\beta}_n^T, \underline{\gamma}_n^T \}^T$$

The amplitude's play the role of discrete generalized coordinates.

Figure 1



PARTITIONED/PERTURBATION INVERSION OF THE  
COEFFICIENT MATRIX

Name the submatrices: 
$$\begin{pmatrix} C_{11} & \vdots & C_{21}^T \\ \dots & \vdots & \dots \\ C_{21} & \vdots & C_{22} \end{pmatrix} \equiv \begin{pmatrix} J & \vdots & H^T \\ \dots & \vdots & \dots \\ H & \vdots & M \end{pmatrix}^{-1}$$

The  $C_{ij}$  can be expressed directly as a function of J, M, H as:

	Form 1	Form 2
$C_{11}$	$J^{-1} - J^{-1} H^T C_{21}$	$(J - H^T M^{-1} H)^{-1}$
$C_{22}$	$(M - H J^{-1} H^T)^{-1}$	$M^{-1} - M^{-1} H C_{21}^T$
$C_{21}$	$-C_{22} H J^{-1}$	$-M^{-1} H C_{11}$

For direct numerical calculations, Form 2 is preferred since

- (i)  $(J - H^T M^{-1} H)$  is a  $3 \times 3$  matrix
- (ii) M is generally diagonally dominant (an identity matrix if one first solves an eigenvalue problem - Note M is positive-definite symmetric)

Figure 3

## CERTAIN REQUIRED PARTIAL DERIVATIVES & HOW TO DETERMINE THEM

### Rotational/Vibrational Equations of Motion

$$\underbrace{\begin{pmatrix} \underline{J}(\underline{\eta}) & \vdots & \underline{H}^T \\ \cdots & \cdots & \cdots \\ \underline{H} & \vdots & \underline{M} \end{pmatrix}}_{\underline{M}(\underline{\eta})} \begin{pmatrix} \dot{\underline{\omega}} \\ \vdots \\ \underline{\dot{\eta}} \end{pmatrix} = \begin{pmatrix} \underline{f}(\underline{\theta}, \underline{\omega}, \underline{\eta}, \underline{\dot{\eta}}, t) + \underline{u}(t) \\ \underline{g}(\underline{\theta}, \underline{\omega}, \underline{\eta}, \underline{\dot{\eta}}, t) \end{pmatrix}$$

or, in inverted form

$$\begin{pmatrix} \dot{\underline{\omega}} \\ \vdots \\ \underline{\dot{\eta}} \end{pmatrix} = \left[ \underline{M}^{-1}(\underline{\eta}) \right] \begin{pmatrix} \underline{f} + \underline{u} \\ \vdots \\ \underline{g} \end{pmatrix}$$

Note

$$\underline{\eta}^T = \{ \eta_1 \quad \eta_2 \quad \dots \quad \eta_n \}$$

$$\frac{\partial}{\partial \eta_i} \begin{pmatrix} \dot{\underline{\omega}} \\ \vdots \\ \underline{\dot{\eta}} \end{pmatrix} = \frac{\partial}{\partial \eta_i} \left[ \underline{M}^{-1} \right] \begin{pmatrix} \underline{f} + \underline{u} \\ \vdots \\ \underline{g} \end{pmatrix} + \underline{M}^{-1} \frac{\partial}{\partial \eta_i} \begin{pmatrix} \underline{f} + \underline{u} \\ \vdots \\ \underline{g} \end{pmatrix}$$

To determine  $\frac{\partial}{\partial \eta_i} \left[ \underline{M}^{-1} \right]$ , observe

$$\underline{M}^{-1} \underline{M} = \underline{I}$$

from which

$$\frac{\partial}{\partial \eta_i} \left[ \underline{M}^{-1} \right] \underline{M} + \underline{M}^{-1} \left[ \frac{\partial \underline{M}}{\partial \eta_i} \right] = 0$$

or

$$\boxed{\frac{\partial}{\partial \eta_i} \left[ \underline{M}^{-1} \right] = -\underline{M}^{-1} \left[ \frac{\partial \underline{M}}{\partial \eta_i} \right] \underline{M}^{-1}}, \quad i=1,2,\dots,n$$

where

$$\left[ \frac{\partial \underline{M}}{\partial \eta_i} \right] = \begin{bmatrix} \frac{\partial \underline{J}(\underline{\eta})}{\partial \eta_i} & \vdots & 0 \\ \cdots & \cdots & \cdots \\ 0 & \vdots & 0 \end{bmatrix}$$

Figure 4

## FORMULATION OF THE OPTIMAL CONTROL PROBLEM

### STATE VARIABLES

$$\underline{x}_1 = \{\theta\}, \quad \underline{x}_2 = \{\eta\}, \quad \underline{x}_3 = \{\omega\}, \quad \underline{x}_4 = \{\dot{\eta}\}$$

### STATE DIFFERENTIAL EQUATIONS

$$\dot{\underline{x}}_1 = [F(\underline{x}_1)] \{\underline{x}_3\} = \underline{F}_1(\underline{x}_1, -, \underline{x}_3, -, -, -)$$

$$\dot{\underline{x}}_2 = \underline{x}_4 = \underline{F}_2(-, -, -, \underline{x}_4, -, -)$$

$$\begin{Bmatrix} \dot{\underline{x}}_3 \\ \dot{\underline{x}}_4 \end{Bmatrix} \equiv \begin{Bmatrix} \{\dot{\omega}\} \\ \{\ddot{\eta}\} \end{Bmatrix} = \begin{Bmatrix} \underline{F}_3(\underline{x}_1, \underline{x}_2, \underline{x}_3, \underline{x}_4, \underline{u}, t) \\ \underline{F}_4(\underline{x}_1, \underline{x}_2, \underline{x}_3, \underline{x}_4, \underline{u}, t) \end{Bmatrix} = \underline{M}^{-1}(\underline{x}_2) \begin{Bmatrix} \underline{f}(\underline{x}_1, t) + \underline{u} \\ \dots\dots\dots \\ \underline{g}(\underline{x}_1, t) \end{Bmatrix}$$

Find  $\underline{u}(t)$  generating a trajectory initiating at  $\underline{x}_1(t_0)$ , terminating at  $\underline{x}_1(t_f)$ , which minimizes the function

$$J = \frac{1}{2} \int_{t_0}^{t_f} (\underline{u}^T W_{uu} \underline{u} + \sum_{i=2}^4 \underline{x}_i^T W_{ii} \underline{x}_i) dt$$

### HAMILTONIAN

$$H = \frac{1}{2}(\underline{u}^T W_{uu} \underline{u} + \sum_{i=2}^4 \underline{x}_i^T W_{ii} \underline{x}_i) + \sum_{i=1}^4 \lambda_i^T \underline{F}_i$$

### PONTRYAGIN'S NECESSARY CONDITIONS

#### Co-state Equations

$$\dot{\lambda}_i = - \frac{\partial H}{\partial \underline{x}_i} \equiv \underline{G}_i(\underline{x}_1, \dots, \underline{x}_4; \lambda_1, \dots, \lambda_4; \underline{u}, t)$$

#### Optimal Control

Minimize  $H$  at each instant with respect to admissible  $\underline{u}(t)$ , this yields  $\underline{u} = \underline{U}(\underline{x}_1, \dots, \underline{x}_4; \lambda_1, \dots, \lambda_4, t)$

Figure 5



## IMBEDDING/RELAXATION METHOD FOR SOLVING TWO-POINT BOUNDARY VALUE PROBLEM

Define merged vector

$$\underline{z} \equiv \{ \underline{x}^T \quad \underline{\lambda}^T \}^T$$

The coupled state and costate differential equations are then

$$\dot{\underline{z}} = [A]\underline{z} + \alpha\{\text{all nonlinear terms}\}$$

- 
- Typically, we know  $\underline{x}(t_0)$  and  $\underline{x}(t_f)$ , but not  $\underline{\lambda}(t_0)$ ,  $\underline{\lambda}(t_f)$ .
  - For  $\alpha = 0$ , we can solve for  $\underline{\lambda}(t_0)$  exactly.
  - By taking sufficiently small  $\alpha$ -increments, we can use converged  $\underline{\lambda}(t_0)$  from neighboring optimal solutions to initiate successive approximations with *arbitrarily good starting estimates* for the unknown  $\underline{\lambda}(t_0)$ .
  - Typically, only 5 to 10 intermediate  $\alpha$ -values are required a practical algorithm results.

Figure 6

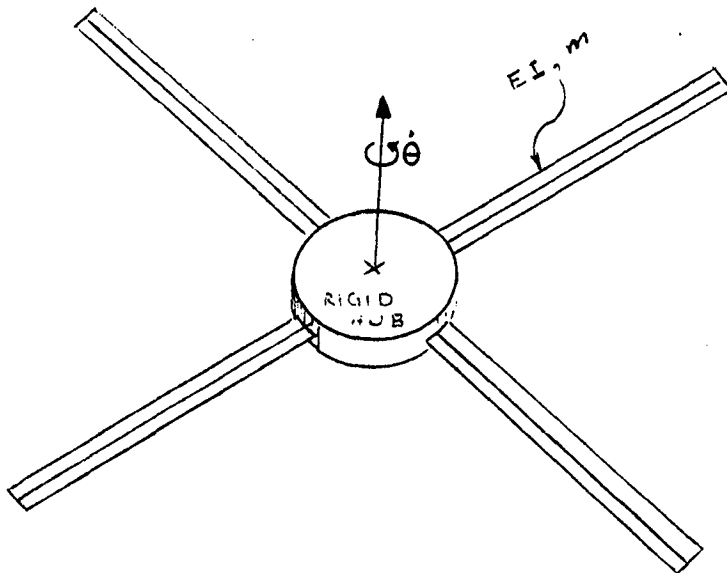


FIGURE 7 UNDEFORMED STRUCTURE

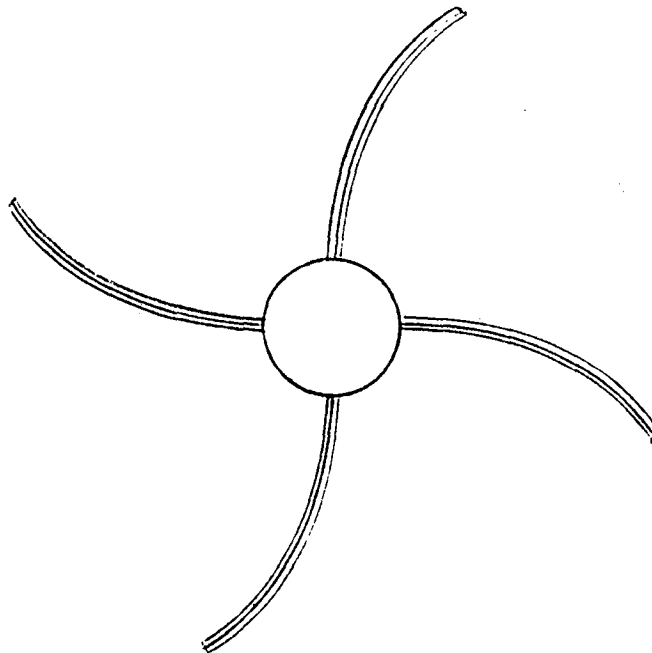


FIGURE 8 ANTISYMMETRIC DEFORMATION

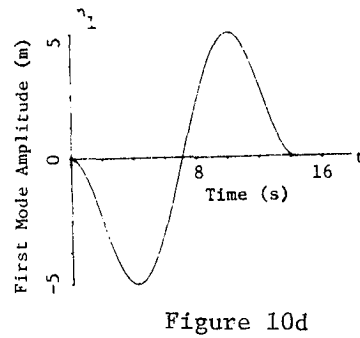
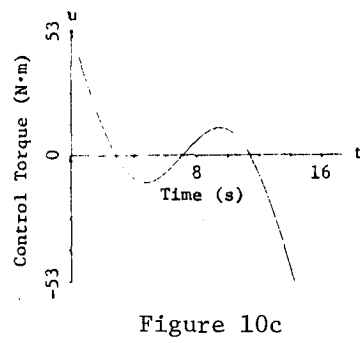
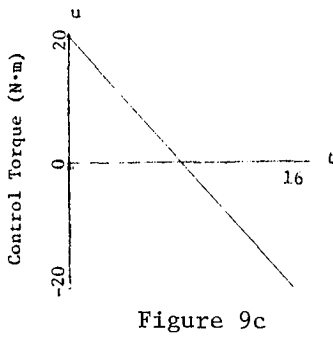
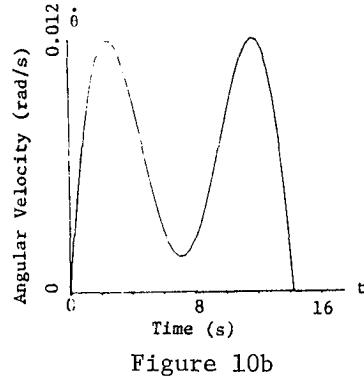
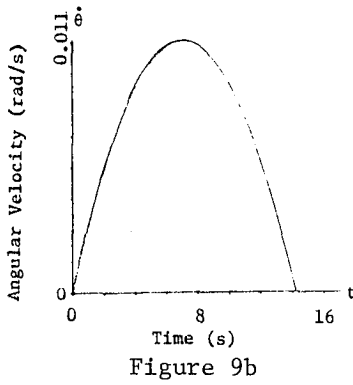
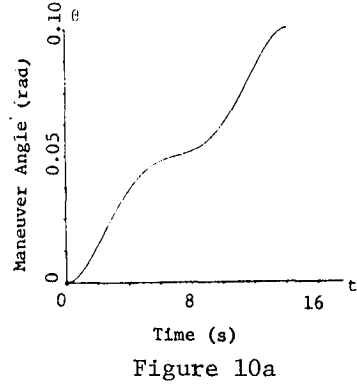
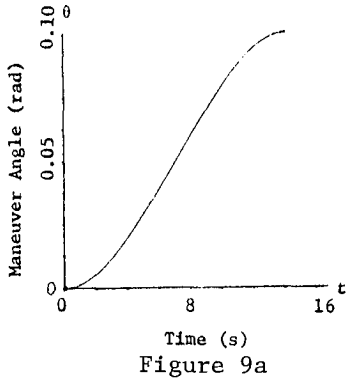


Figure 9 Case 1 Rigid Body Rest-To-Rest Maneuver

Figure 10 Cases 2L, 2N Flexible Appendages Rest-To-Rest Maneuver  $t_f = 2\pi/\omega_1$

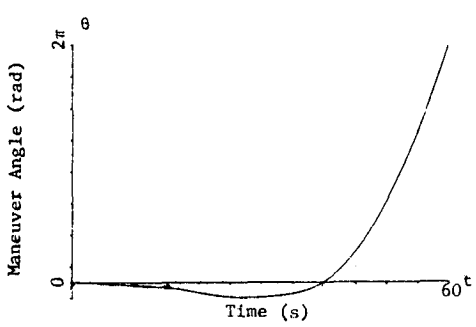


Figure 11a

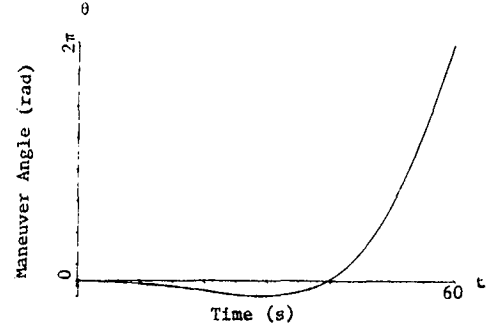


Figure 12a

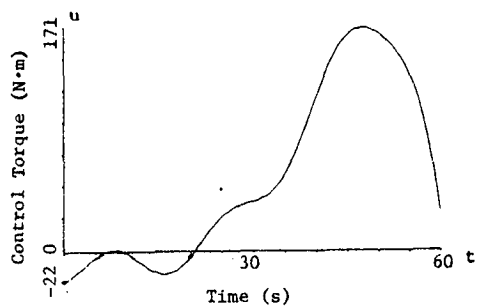


Figure 11b

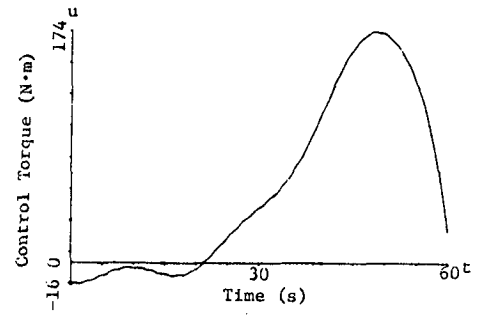


Figure 12b

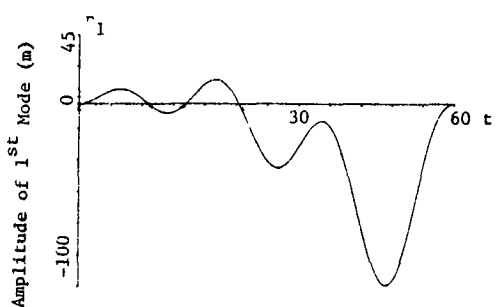


Figure 11c

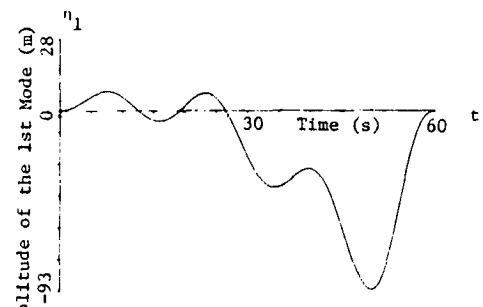


Figure 12c

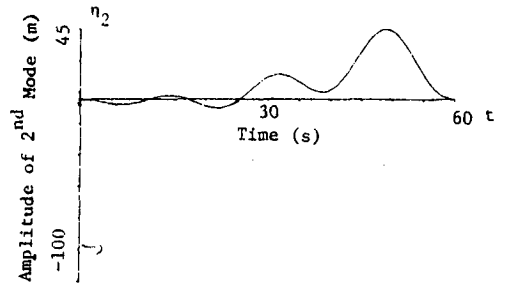


Figure 11d

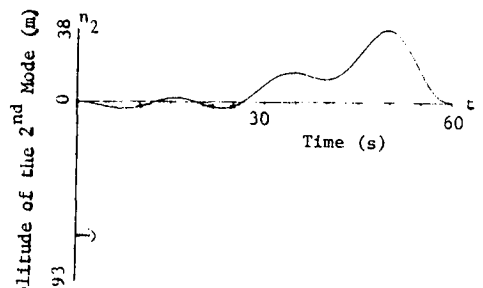


Figure 12d

Figure 11 Case 3L Linear Spinup Maneuver

Figure 12 Case 3N Nonlinear Spinup Maneuver

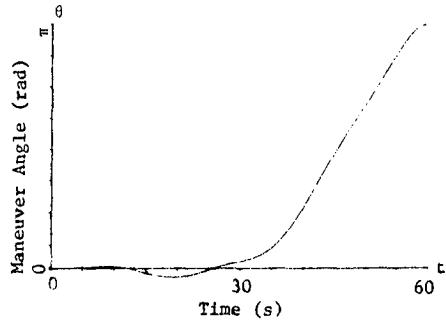


Figure 13a

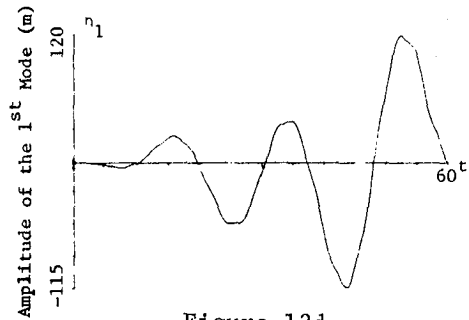


Figure 13d

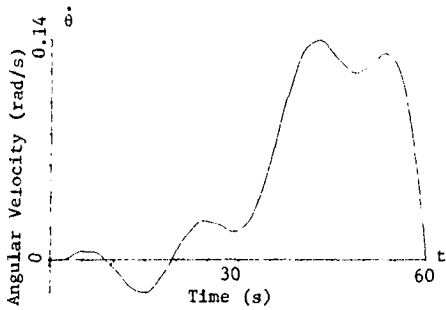


Figure 13b

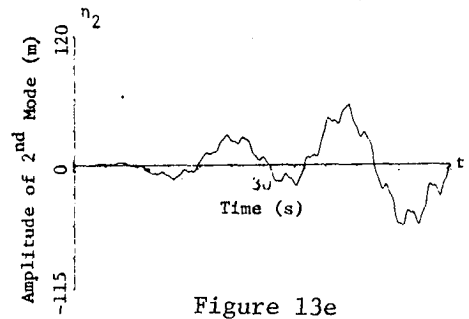


Figure 13e

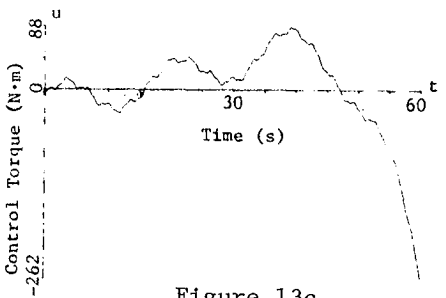


Figure 13c

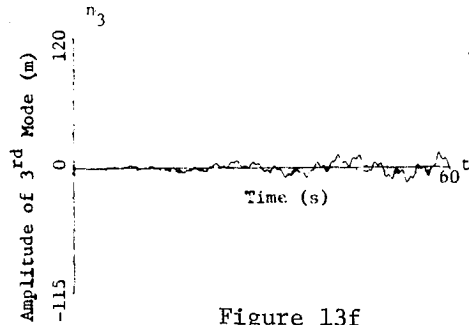


Figure 13f

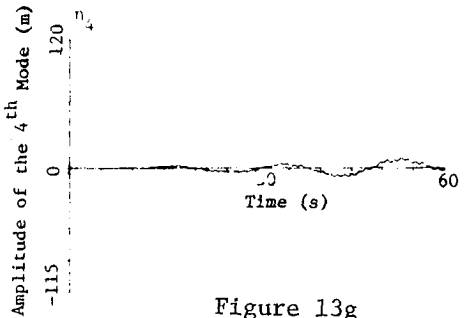


Figure 13g

Figure 13 Case 4L Rest-To-Rest Maneuver  
Controlling and Arresting 4 Modes

TABLE 1 DESCRIPTION OF TEST CASE MANEUVERS

Case #	Qualitative Description	# of Modes (N)	$\theta_o$ (RAD)	$\dot{\theta}_o$ (RAD/SEC)	$\theta_f$ (RAD)	$\dot{\theta}_f$ (RAD/SEC)	$W_{uu}$	$W_{ss}$
1	Rigid Appendages Rest-to-Rest Maneuver $t_f = 14.221$ sec.	0	0	0	0.1	0	1.0	[0]
2L	Linear Kinematics Rest-to-Rest Maneuver $t_f = 2\pi/\omega_1 = 14.221$ sec	1	0	0	0.1	0	1.0	[I]
2N	Nonlinear Kinematics Rest-to-Rest Maneuver $t_f = 2\pi/\omega_1 = 14.221$ sec	1	0	0	0.1	0	1.0	[I]
3L	Linear Kinematics Spinup Maneuver $t_f = 60$ sec	2	0	0	$2\pi$	0.5	1.0	[I]
3N	Nonlinear Kinematics Spinup Maneuver $t_f = 60$ sec	2	0	0	$2\pi$	0.5	1.0	[I]
4L	Linear Kinematics Rest-to-Rest Maneuver $t_f = 60$ sec	4	0	0	$\pi$	0	1.0	[I]
4N	Nonlinear Kinematics Rest-to-Rest Maneuver $t_f = 60$ sec	4	0	0	$\pi$	0	1.0	[I]